Studies on Impact of Electron Cyclotron Wave Injection on the Internal Transport Barriers on JT-60U

S. Ide, H. Takenaga, A. Isayama, Y. Sakamoto, M. Yoshida, C. Gormezano and the JT-60 Team

Japan Atomic Energy Agency,
Naka, Ibaraki-ken, 311-0193 Japan

e-mail contact of main author: ide.shunsuke@jaea.go.jp

Abstract. Impact of the electron cyclotron range of frequency wave (ECRF) on the internal transport barriers (ITBs) in a weak shear (WS) plasma has been investigated in JT-60U. The fundamental O-mode ECRF of 110 GHz injected obliquely (co-current drive) from the low field side is used. It is observed that the ion temperature ($T_{\rm i}$) ITB in a WS plasma can be degraded by ECRF. It is clarified for the first time that the degradation depends increasingly on the EC power ($P_{\rm EC}$) but decreasingly on the plasma current ($I_{\rm p}$). Moreover it is confirmed that ECRF affects the toroidal rotation ($V_{\rm t}$) indirectly and results in flattening of $V_{\rm t}(\rho)$ and therefore the radial electric field ($E_{\rm r}$) profiles regardless of the direction of the target $V_{\rm t}(\rho)$, peaking co or counter direction (relative to the $I_{\rm p}$ direction). Furthermore, it is newly found that $T_{\rm i}$ and $V_{\rm t}$ in the whole ITB region are affected with almost no delay from the EC onset even with off-axis EC deposition. These results indicate that the EC injection unveiled a semi-global structure that characterizes $T_{\rm i}$ ITB in a WS plasma.

1. Introduction

In ITER advanced operations and a steady-state tokamak reactor, the internal transport barriers (ITBs) are expected to play an important role in confinement improvement and in increasing the bootstrap current fraction. In many tokamaks, formation of ITBs has been observed and contributed to improving performance. A weak magnetic shear (WS) ITB plasma with the safety factor (q) at the plasma center (q_0) slightly above unity can be a good candidate for the ITER hybrid scenario and even for an attractive operational scenario in a reactor. In JT-60U, the so called high $\beta_{\rm p}$ plasma [1] is in this category. However it has been observed that the ion temperature ($T_{\rm i}$) ITB in a WS plasma can be degraded by injection of the electron cyclotron range of frequency wave (ECRF) [2–4]. Since ECRF directly heats electrons, this phenomenon can be a critical issue in a burning plasma where electron heating is predominant. Even if this phenomenon is intrinsic to ECRF, this should be avoided. Because localized current drive by ECRF is believed to be one of the best ways to suppress the neo-classical tearing modes (NTM), which can be destabilized in an ITER hybrid discharge with the ITBs for example, and affect overall performance. Therefore understanding of this phenomenon and identification of the operational space for this phenomenon to occur are important issues not only for plasma physics but also for fusion development. This paper is to understand dependences of this phenomenon on plasma and operational parameters and to investigate underlying physics. In this paper, experimental setup (heating system and key diagnostics) is described in the section 2, the experimental results are described in the section 3 and finally conclusions are given in the section 5.

2. Experimental Setup

The target plasma is produced with positive ion source neutral beam (P-NB) of which beam acceleration energy is about 85 keV. In JT-60U P-NBs of various injection geometries are installed. They are consist of; two tangential beams directing the same direction as that of the plasma current (CO-beams) and two tangential beams directing opposite to the plasma current (CTR-beams), and one of each beams in the same direction is almost on-axis deposition and the other is off-axis deposition, seven perpendicular beams, four of them are almost on-axis deposition and the others are off-axis deposition. The power source of the ECRF systems is four gyrotrons of 110 GHz, which corresponds to the fundamental electron cyclotron harmonics in the experiments discussed in this paper. Each gyrotrons feed power through independent transmission lines, but three of them (EC unit #1 to #3) share the same antenna mirror. This mirror enables steering of the beams in the poloidal cross section, but not in the toroidal direction. The toroidal injection angle is fixed, so these three beams always drives current. The power from the other gyrotron (EC unit #4) is injected through independent mirror which enables steering both in poloidal and toroidal directions. Therefore, this beam line can be used for both co and counter current drive and pure heating. The polarization of the injection wave can be changed. In all the experiments shown in this paper, the polarization of the wave is the O-mode. The key diagnostic in this experiment is charge exchange recombination spectroscopy (CXRS) measurement. In particular a CXRS system, which has been installed recently and enables fast (typically 200 Hz/5 ms) sampling and provides detailed information on changes in a small time scale.

3. Experimental Results

This section describes experimental results of the influence of ECRF on the T_i ITB in JT-60U WS plasmas.

3.1. Typical Response of the Ion Temperature ITB to the EC Injection and the EC Power

Waveforms of a typical discharge (plasma current I_p = 1.0 MA, toroidal magnetic field at the plasma major radius B_{t0} = 3.7 T) are shown in Fig. 1. With NB injection of about 10 MW, target high β_p plasma is formed. As shown in the figure, central T_i decreases with injection of ECRF. The influence of the ECRF is higher as the EC power (P_{EC}) increases. This can be seen in Fig. 2 where changes in the T_i profile are plotted. Before ECRF injection, a clear ITB structure is seen in the T_i profile. As ECRF is injected and the power increases, the gradient of the T_i at the ITB region ($\rho <\sim 0.5$) decreases. With P_{EC} = 2.17 MW the ITB structure is almost vanished. Change in the electron temperature (T_e) profile is also shown in Fig. 2. With the EC injection, T_e increases but not largely as P_{EC} increases. This may suggest that transport of T_e is also affected as the transport of T_i is enhanced. In the discharge shown in the figure, P_{EC} was scanned stepwise up and down, but not completely to zero. This is due to stop of the NB power due to shine through. It should be noted here that with shorter EC pulses, it has been observed the T_i ITB recoverd to the almost initial strength. This indicates that the impact of the ECRF is

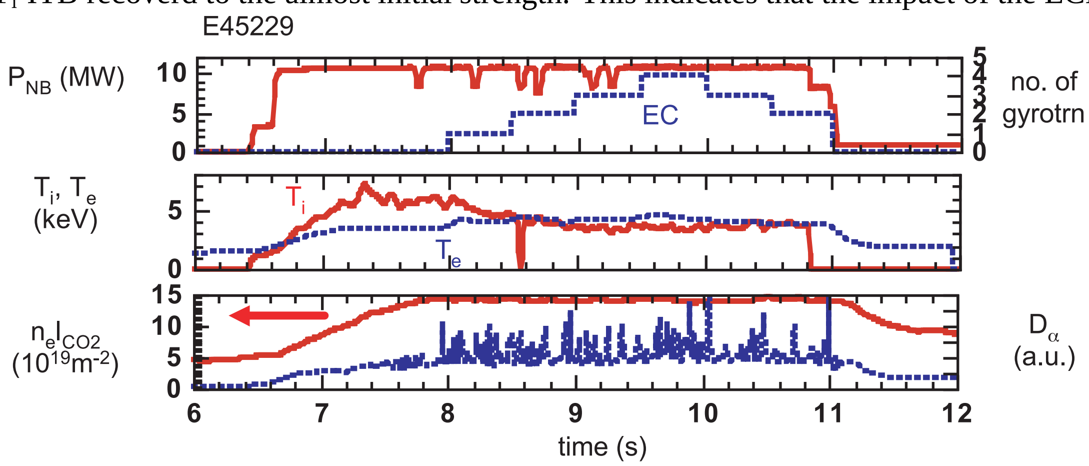

FIG. 1. Typical waveforms (E45229). (a) the NB power (P_{NB}) and number of EC power source (gyrotron), (b) the ion and electron temperatures (T_i and T_e) near the plasma center. (c) the line integrated electron density ($n_\mathrm{e}l$, path length is about 5.7 m) and the brightness of the D_α line.

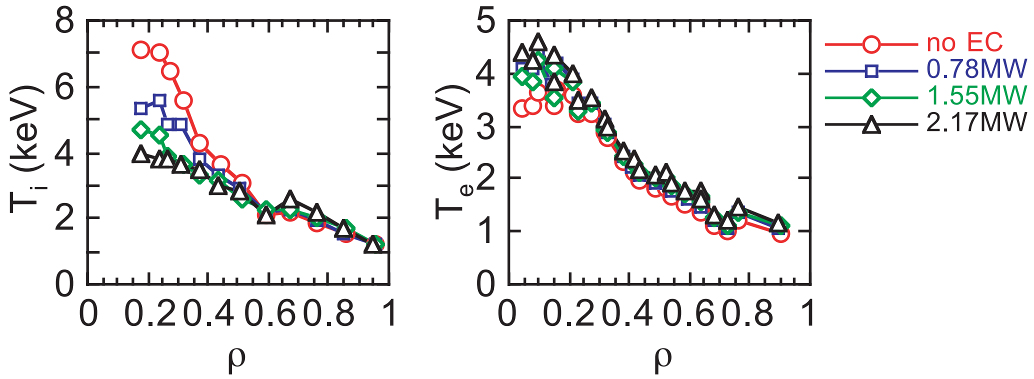

FIG. 2. Change in the T_i and the T_e profiles with various injected EC power (P_EC) in the same discharge shown in Fig. 1.

not fatal but recoverable. In other words, this can be applied to change the ITB strength with P_EC.

3.2. Effect of the Magnitude of the Plasma Current and Effect of the EC Current Drive

The impact of ECRF injection has been investigated on plasmas with different I_p. It is found that the impact of ECRF is different as I_p changes. In Fig. 3 (a) plotted are the changes in the T_i gradient in the ITB region ($\rho \lesssim 0.4$) with P_EC for various I_p (1.0, 1.2 and 1.4 MA). The change in the T_i profile plotted in Fig. 2is indicated with open circles in Fig. 3 (a). As seen in the figure, the impact becomes smaller at high I_p. Changes in the T_i profile with $P_\mathrm{EC} \sim 1.5$ MW injection for both I_p = 1.0 and 1.2 MA are shown in Fig. 3 (b) and (c). At I_p = 1.2 MA, change in the T_i gradient at the ITB region is very small compared to that at I_p = 1.0 MA case.

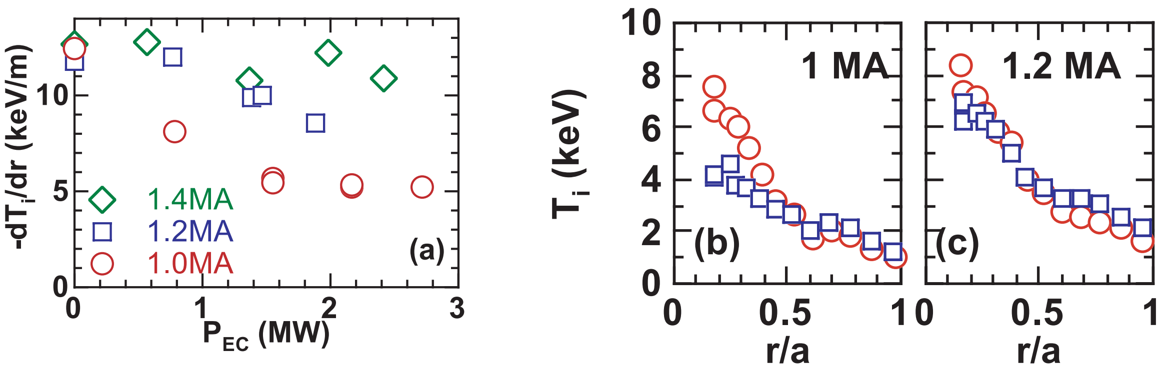

FIG. 3. Impact of ECRF on T_i ITB for different plasma current. (a) Change in the T_i gradient against injected EC power (P_EC) for plasmas of I_p = 1.0 (open circles), 1.2 (open squares) and 1.4 MA (open diamonds). Changes in the T_i profile with EC injection for I_p = 1.0 MA (b) and 1.2 MA (c).

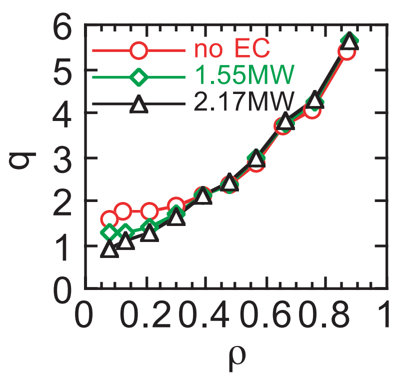

FIG. 4. Change in the q profile with various EC power in the same discharge shown in Fig. 1.

In all the experiments shown above, the toroidal injection angle of EC #4 was set to current drive mode so that all the EC units were to drive current in positive direction. This fact and the result of I_p dependence could suggest that the cause of this T_i ITB degradation effect by ECRF could be attributed to a change in the current profile due to the EC current drive. However, experimental data indicate that is the case. The safety factor profiles in E45229 with P_EC = 0, 0.78 and 1.55 MW are plotted in Fig. 4. It is clear that q in the central region decreases as P_EC increases, and this should be attributed to

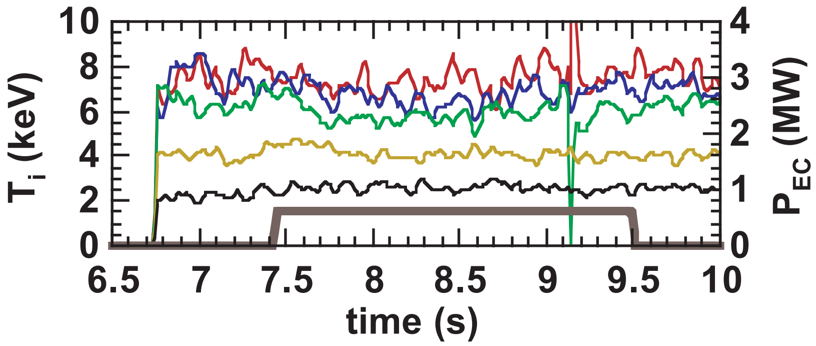

FIG. 5. Temporal evolution of T_i at various locations with pure ECH. Although the change is small due to small injection EC power (~0.62 MW, decrease in the core T_i can be observed.

ECCD. However, the change is limited in a narrow region (ρ <0.4), while the ITB extend up to ρ = 0.5-0.6 and the whole ITB region is affected. In order to clarify the effect of the current drive, pure ECH was applied. As described in section 2, one EC unit can be operated with the toroidal injection angle = 0 degree, that is pure electron heating mode. Although the change was small, a clear T_i degradation, within the ITB region, was observed with only one EC unit in heating mode for even a smaller power (0.62 MW) as shown in Fig. 5. This result clearly indicates that the current drive is not the key for the T_i ITB degradation.

3.3. Effect on Different Toroidal Rotation Profile Plasmas

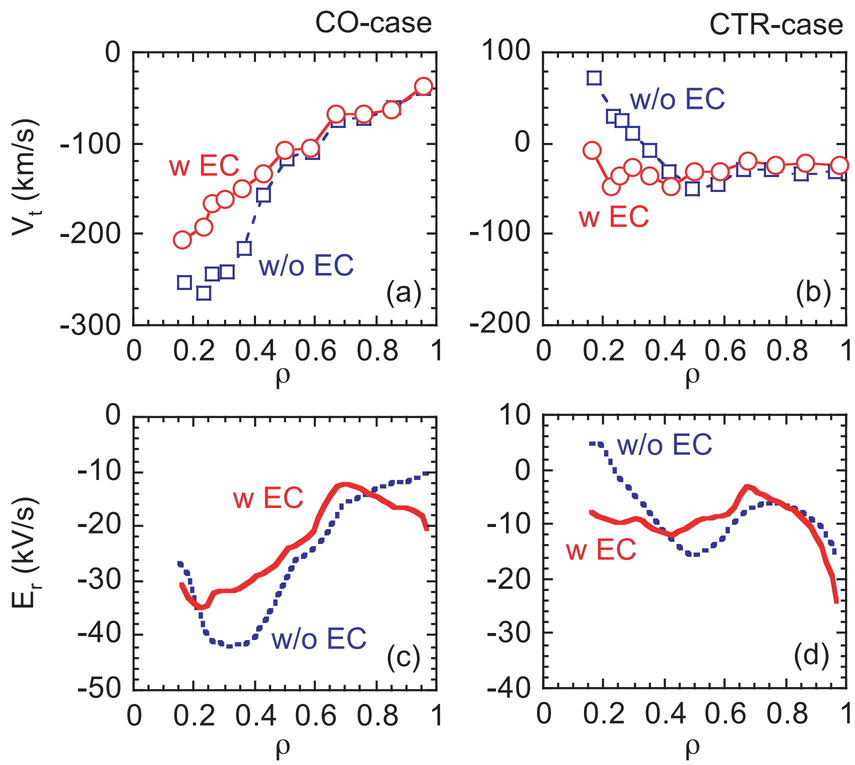

FIG. 6. Comparison of change in the toroidal rotation velocity (V_t) and the radial electric field (E_r) profiles for different target V_t profiles. A target V_t profile with CO-dominant; (a) and (c), and CTR-dominant; (b) and (d). The target profiles before EC injection are shown with open squares in (a) and (b) and dashed lines in (c) and (d), while those with the EC injections are shown with open circles and solid lines. These target plasmas were prepared by changing combination of tangential beams. In both cases, the V_t profile is found to be flattened by the EC injection.

In the previous study [3], it was found that the toroidal rotation (V_t) profile changed (became flattened) and so did the radial electric field (E_r) profile with the injection of ECRF. However, it was not clear whether ECRF directly rotated the plasma or not. In order to clarify it, different target V_t profiles were prepared in a 1 MA plasma (B_{t0} = 3.7 T) utilizing co or counter tangential NBs. After installation of the ferritic steel on the JT-60U first wall, $V_t(\rho)$ can be changed wider than before by changing combination of the tangential NBs [5, 6]. With co-NB, a V_t profile that peakes towards co-direction was obtained, while with counter-NB the V_t profile peaked towards counter (open squares in Fig. 6 (a) and (b)). As ECRF is injected, V_t in the core region changed, but oppositely. As the result the V_t profile became flatter in both cases as shown in Fig. 6 (a) and (b) (open circles). Since the change in the V_t profile is opposite in these cases, it can be concluded that ECRF does not change the V_t profile directly, but indirectly. Flattening of the V_t profile indicates flattening of the E_r profile, as shown in Fig. 6 (c) and (d) (before the EC injection; dashed line and during the EC injection; solid line). It should be noted that in the P_{EC} scan (Fig. 1 and Fig. 3), the V_t profile was found to become flatter as the T_i gradient decreased.

3.4. Off-axis EC Deposition

The results described above were obtained with on-axis EC deposition. For comparison, off-axis (ρ ~0.4) but yet inside ITB EC deposition was carried out using a steering mirror at the same B_t. It was found that a P_{EC} ~2.1 MW off-axis injection also degrades T_i ITB as shown in Fig. 7 (a), and the change is almost the same as that with P_{EC} ~1.5 MW on-axis deposition. In Fig. 7 (b) are plotted the temporal evolution of T_e measured by the electron cyclotron emission (ECE) polychromator for both on- and off-axis deposition cases. Difference in deposition is clearly shown in the figure. Furthermore, new and very interesting observation was obtained. In Fig. 7 (b) and (c), T_i and V_t waveforms at $\rho \sim$ 0.2 are shown for both off- (solid lines) and on-axis (dashed lines) deposition. As clearly seen, both T_i and V_t near axis start changing at the EC onset even with off-axis deposition.

In order to investigate changes in T_i and V_t in faster time scale, the new CXRS diagnostics system that has better time resolution was utilized. The target plasma is again a high β_p plasma of I_p = 1 MA at B_{t0} = 3.7 T with $P_{NB} \sim$ 8 MW. It should be noted that the plasma having no clear ELMs is likely to be in an L-mode regime. The deposition was changed by the steering mirrors as well, and the EC deposition in this plasma was $\rho \sim$ 0.35. Temporal evolutions of T_i and V_t with fast sampling time (5 ms) at several locations (not all the measuring locations) are shown in Fig. 8. After EC injection at ~7.42 s, both T_i and V_t start to change as shown in the figures. Evolutions of T_i and V_t at the nearest to the EC deposition are indicated with solid lines in the figures.

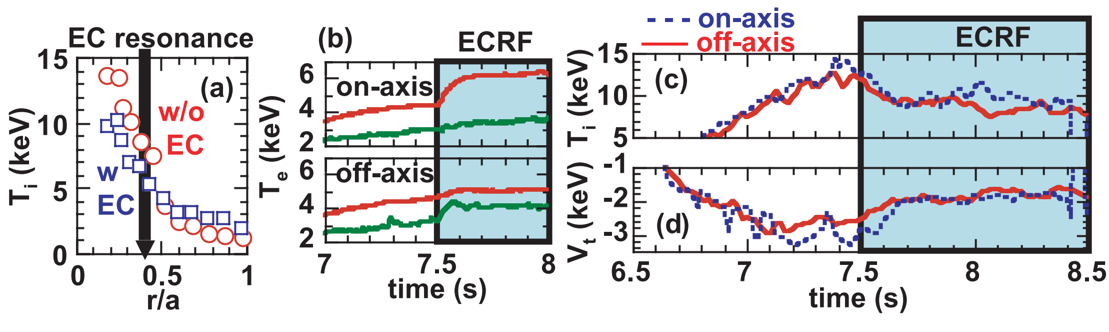

FIG. 7. An off-axis EC deposition case. (a) Change in the T_i profile with EC injection, the EC deposition is schematically shown. (b) Comparison of temporal evolutions of the ECE signal at near center and $\rho \sim$ 0.4 for on- and off-axis deposition cases. Difference in the deposition is clearly shown. (c) Comparison of temporal evolutions of the core T_i and V_t for on- and off-axis deposition cases. Although the deposition is different, no clear delay is seen in the waveforms both for T_i and V_t.

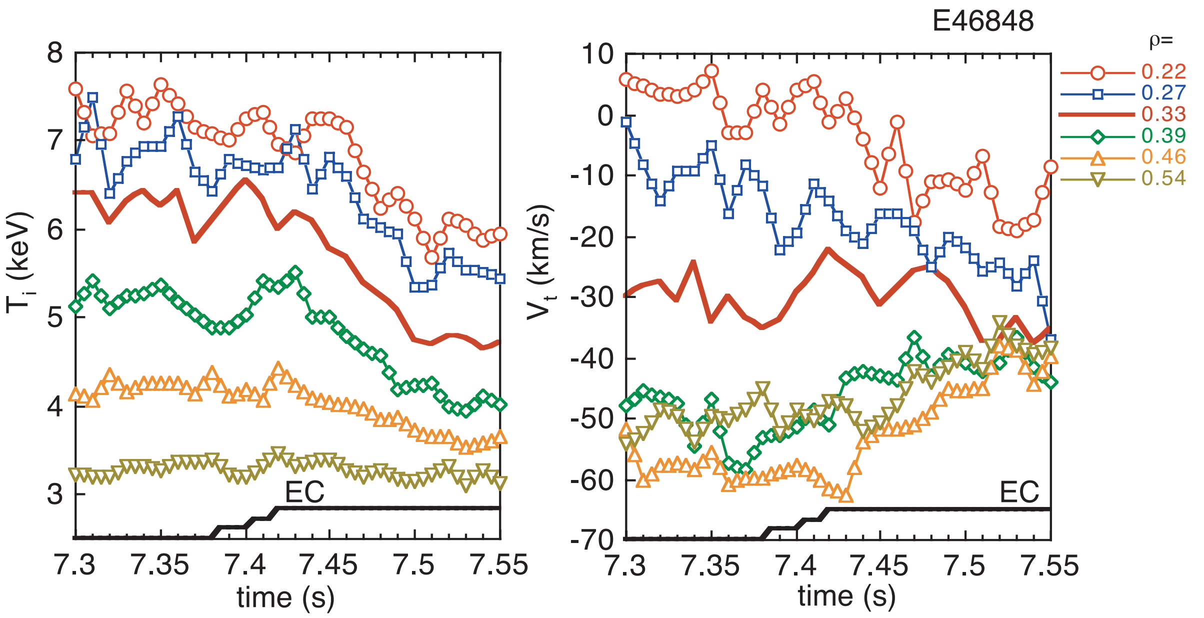

FIG. 8. Temporal evolutions of $T_{\rm i}$ and $V_{\rm t}$ at various locations measured with fast sampling CXRS with $P_{\rm EC}$ MW injection. The change in both $T_{\rm i}$ and $V_{\rm t}$ is measured with a sampling time of 5 ms.

It is not very clear if there is any delay of change in $T_{\rm i}$ and $V_{\rm t}$ at remote locations from the EC deposition.

In order to clarify if there is a delay or not in $T_{\rm i}$ changes, $T_{\rm i}$ at various locations are plotted against $T_{\rm i}$ at ρ = 0.33 (the EC deposition) during 7.41 and 7.50 s, just around the start of the change due to the EC injection, in Fig. 9. In order to avoid overlap of plots, $T_{\rm i}$s at ρ = 0.22 (there are two measuring points both side of the plasma center) are plotted in a separated box (upper figure). As $T_{\rm i}$ decreases almost monotonously, a trace of $T_{\rm i}$ from the right-hand side to the left-hand side corresponds to a current of time. As shown in the figure, $T_{\rm i}$ at ρ = 0.22 (there are two measurement points), 0.50 and 0.54 look to change with a delay of about 50 ms (about ten data points) to $T_{\rm i}$ at the EC deposition. It should be noted that the foot of the $T_{\rm i}$ ITB locates at around $\rho \sim 0.5$ On the other hand, though data scatter somehow, $T_{\rm i}$ at 0.25 $\leq \rho \leq$ 0.46 look to change with almost no delay to $T_{\rm i}$ at ρ = 0.33. Unfortunately, no measurement was available at ρ <0.22 for this plasma configuration. Therefore, it is not possible to obtain information on the structure in that core region. Concern-

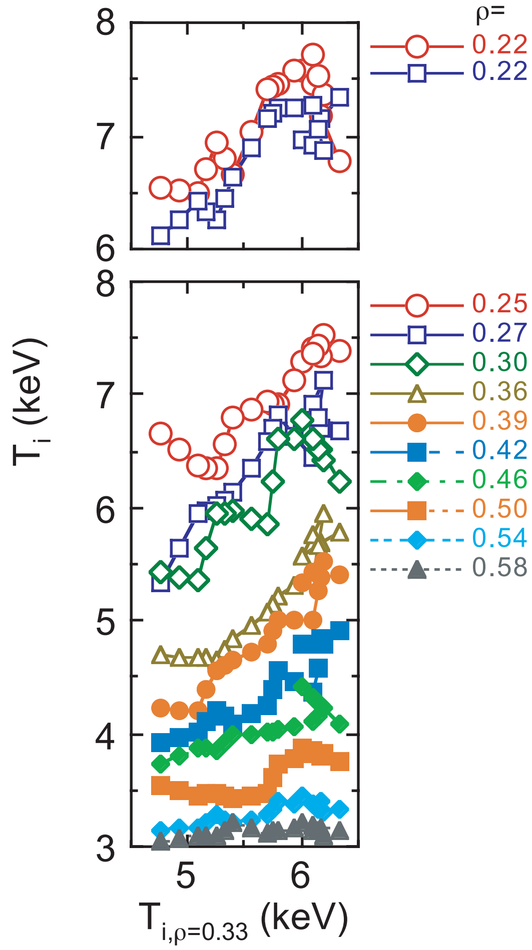

FIG. 9. Evolution of $T_{\rm i}$ at various locations (ρ = 0.22–0.58) against $T_{\rm i}$ at ρ = 0.33, near the EC deposition. $T_{\rm i}$ at the two center most channels (ρ = 0.22) are plotted separately in the top box, in order to avoid overlap of plots. Data in a time duration from 7.41 to 7.50 s are plotted. Since $T_{\rm i}$ decreased as the EC power was injected, movement from the right hand side to the left hand side corresponds to temporal evolution.

ing the change in V_t, it is difficult to apply the same way since, as it can be found in Fig. 8, V_t at ρ = 0.33 does not change quickly as T_i at the same location or V_t at other location does. This is because, with EC injection, These results indicate that in the region of 0.25 $\leq \rho \leq$ 0.46, or a bit wider but surely narrower than 0.22 $<\rho<$0.50, ECRF affects non-locally on a certain semi-global structure, which could be determining the T_i ITB. This is for the first time that such a semi-global structure is confirmed in a weak shear ITB plasma. Due to off-axis deposition, changes in T_e and j were smaller than those observed in the on-axis deposition cases. This indicates that direct effect by T_e or j could be excluded. On the other hand, the results indicate correlation with V_t or E_r as discussed previously [3]. Underlying physics will be discussed with emphasis on changes in E_r (r).

4. Conclusion

Effect of ECRF on T_i ITB in a weak shear plasma was investigated. Injection of ECRF entails a degradation of the T_i ITB. It is shown that the effect increases as the injected EC power increases. It is also shown that the effect becomes smaller for a higher I_p plasma. Although the reason is not clear yet, current drive by ECRF seems not to be responsible for this effect. It seems that EC injection affects the V_t and presumably the E_r profiles. With ECRF injection, the V_t profile is flattened no matter the direction the target V_t profile peaks. This indicates that EC injection influences the background structure, the E_r profile or the ITB structure, directly. Moreover, it is shown that the effect on the T_i ITB is less sensitive to the EC deposition. Degradation of the T_i ITB occurs no matter if the EC deposition is on-axis or off-axis, though the injection power necessary to have the same effect is different, higher power would be required for off-axis deposition. Within the time resolution of 5 ms, no clear delay was observed in both T_i and V_t signal in the ITB region. This indicates that ECRF is acting on a certain background structure which has a semi-global nature. This work would contribute to identify the operational region where the T_i ITB degradation can be avoided when ECRF is utilized NTM suppression. However on the other hand, this effect can be utilized for ITB control. Smooth and continuous dependence without hysteresis on P_EC is preferable for control and insensitivity to deposition do not require the precision linked to spatial control. ECRF can be a more realistic tool than others such as the V_t profile control in a burning plasma. A fundamental physics mechanism which plays the main role in this phenomenon is not clear yet. It is not clear even if this is intrinsic to ECRF or not. Detailed comparison with other electron heating schemes, such as negative ion source NB injection or lower hybrid wave heating, would be necessary in future work.

Acknowledgement

The authors would like to acknowledge Drs. S. Moriyama, M. Seki and T. Fujii for discussion and operation of the ECRF system, and all those who have contributed to the operation of the JT-60U system. This research was partially supported by Japan Society for the Promotion of Science under Grant-in-Aid for Scientific Research (C) 18560798.

References

[1] Kamada Y., *et al.*, Nucl. Fusion **34**, 1605 (1994).
[2] Ide S., *et al.*, Plasma Phys. & Controlled Fusion **44**, A137 (2002).
[3] Ide S., *et al.*, Nucl. Fusion **44**, 87 (2004).
[4] Greenfield C. M., *et al.*, Nucl. Fusion **39**, 1723 (1999).
[5] Shinohara K. *et al.*, this conference, FT/P5-32 .
[6] Yoshida M. *et al.*, this conference, EX/P3-22 .